THE JOURNAL OF BIOLOGICAL CHEMISTRY
Vol. 276, No. 43, Issue of October 26, pp. 39892–39897, 2001
Printed in U.S.A.

IGF-I Receptor-induced Cell-Cell Adhesion of MCF-7 Breast Cancer Cells Requires the Expression of Junction Protein ZO-1*

Received for publication, July 16, 2001
Published, JBC Papers in Press, August 22, 2001, DOI 10.1074/jbc.M106673200

Loredana Mauro‡§, Monica Bartucci‡§, Catia Morelli‡§, Sebastiano Ando'§, and Eva Surmacz‡¶

From the ‡Kimmel Cancer Center, Thomas Jefferson University, Philadelphia, Pennsylvania 19107 and the §Department of Cellular Biology and Faculty of Pharmacy, University of Calabria, 87030 Rende, Italy

Hyperactivation of the insulin-like growth factor I receptor (IGF-IR) contributes to primary breast cancer development, but the role of the IGF-IR in tumor metastasis is unclear. Here we studied the effects of the IGF-IR on intercellular connections mediated by the major epithelial adhesion protein, E-cadherin (E-cad). We found that IGF-IR overexpression markedly stimulated aggregation in E-cad-positive MCF-7 breast cancer cells, but not in E-cad-negative MDA-MB-231 cells. However, when the IGF-IR and E-cad were co-expressed in MDA-MB-231 cells, cell-cell adhesion was substantially increased. The IGF-IR-dependent cell-cell adhesion of MCF-7 cells was not related to altered expression of E-cad or α-, β-, or γ-catenins but coincided with the up-regulation of another element of the E-cad complex, zonula occludens-1 (ZO-1). ZO-1 expression (mRNA and protein) was induced by IGF-I and was blocked in MCF-7 cells with a tyrosine kinase-defective IGF-IR mutant. By co-immunoprecipitation, we found that ZO-1 associates with the E-cad complex and the IGF-IR. High levels of ZO-1 coincided with an increased IGF-IR/α-catenin/ZO-1-binding and improved ZO-1/actin association, whereas down-regulation of ZO-1 by the expression of an anti-ZO-1 RNA inhibited IGF-IR-dependent cell-cell adhesion. The results suggested that one of the mechanisms by which the activated IGF-IR regulates E-cad-mediated cell-cell adhesion is overexpression of ZO-1 and the resulting stronger connections between the E-cad complex and the actin cytoskeleton. We hypothesize that in E-cad-positive cells, the IGF-IR may produce antimetastatic effects.

The insulin-like growth factor I (IGF-I)[1] receptor (IGF-IR) is a ubiquitous tyrosine kinase capable of regulating different growth-related and -unrelated processes (1–3). Recent evidence indicates that the IGF-IR may be involved in breast cancer development. The IGF-IR is significantly (10–14-fold) overexpressed in estrogen receptor-positive primary breast tumors compared with normal mammary epithelium or benign tumors (1, 4). Moreover, the intrinsic ligand-independent tyrosine kinase activity of the IGF-IR has been found to be substantially up-regulated (~2–4-fold) in breast cancer cells (4). It has been suggested that the increased receptor function coupled with enhanced receptor expression amounts to a 40-fold elevation in IGF-IR activity in estrogen receptor-positive breast tumors (4). Recent clinical and experimental data indicate that up-regulation of IGF-IR signaling in estrogen receptor-positive breast cancer cells is associated with autonomous cell proliferation, estrogen-independence, and increased resistance to various antitumor treatments (1). Consequently, it is believed that hyperactivation of the IGF-IR may induce and sustain the growth of primary breast tumors (1).

The role of the IGF-IR in breast cancer metastasis, however, is unclear. The experimental data suggest that the IGF-IR has a function in cell spreading by effectively stimulating the motility of different metastatic breast cancer cell lines lacking the expression of a major adhesion protein, E-cadherin (E-cad) (1, 5, 6). On the other hand, we and others have shown that in more differentiated E-cad-positive cells, IGF-I treatment or IGF-IR overexpression up-regulates cell-cell adhesion, which correlates with increased cell survival in three-dimensional culture and with reduced cell migration *in vitro* and in organ culture (1, 7–10).

The mechanism of IGF-I-dependent intercellular adhesion and the clinical consequences of this phenomenon have not been fully elucidated. Previously, we demonstrated that in MCF-7 human breast cancer cells, the IGF-IR co-localizes and co-precipitates with the E-cad complex and that IGF-induced aggregation is blocked with an anti-E-cad antibody (7). In this study we assessed the effects of the IGF-IR on the elements of the E-cad adhesion complex, *i.e.* E-cad; β-, γ-, and α-catenins; and α-catenin-associated proteins (see Fig. 6). The initial results prompted us to focus on an α-catenin-binding element, the junction protein zonula occludens-1 (ZO-1).

ZO-1 is a ~220-kDa scaffolding protein containing various domains (an SH3 domain, three PDZ domains, a proline-rich region, and a guanylate kinase domain) that allow its interaction with specialized sites of plasma membrane as well as with other proteins (11, 12). ZO-1 is a characteristic element of tight junctions, but recently its presence has also been demonstrated in E-cad adherens junctions (13–15). The role of ZO-1 in adherens junctions is yet unclear, but it is assumed that it may functionally link E-cad with the actin cytoskeleton because it associates with α-catenin and actin through its N and C terminus, respectively (Ref. 13, see Fig. 6). In addition, as a member of the membrane-associated guanylate kinase homologue (MAGUK) family of putative signaling proteins, ZO-1 may be involved in signal transduction. Indeed, ZO-1 has been found to

* This work was supported by United States Department of Defense Grants DAMD1799-1-9407 and DAMD17-97-1-7211, International Union Against Cancer (ICRETT) Award 1007/1999, and Programma Operativo Plurifondo 98, Regione Calabria. The costs of publication of this article were defrayed in part by the payment of page charges. This article must therefore be hereby marked "*advertisement*" in accordance with 18 U.S.C. Section 1734 solely to indicate this fact.

¶ To whom correspondence should be addressed: Kimmel Cancer Center, Thomas Jefferson University, 233 S. 10th St., BLSB 631, Philadelphia, PA 19107. Tel.: 215-503-4512; Fax: 215-923-0249; E-mail: eva.surmacz@mail.tju.edu.

[1] The abbreviations used are: IGF-I, insulin-like growth factor I; IGF-IR, IGF-I receptor; E-cad, E-cadherin; ZO-1, zonula occludens-1 junction protein; Y3F, Tyr-1131, Tyr-1135, and Tyr-1136 replaced with Phe; WB, Western blotting or Western blotted; pAb, polyclonal antibody; mAb, monoclonal antibody; ERK1, extracellular signal-related kinase 1; IRS-1, insulin receptor substrate 1; MAPK, mitogen-activated protein kinase.

TABLE I

Effects of IGF-IR and ZO-1 expression on cell aggregation in E-cad-positive and -negative breast cancer cells

The stable cell lines (MCF-7, MCF-7/IGF-IR, MCF-7/IGF-IR/anti-ZO-1, MCF-7/Y3F, MDA-MB-231, and MDA-MB-231/IGF-IR) and transiently transfected populations (MDA-MB-231/E-cad, MDA-MB-231/vector, MDA-MB-231/IGF-IR/E-cad, and MDA-MB-231/IGF-IR/vector) were cultured as three-dimensional spheroids in normal growth medium. The number of spheroids of different sizes was established as described under "Materials and Methods." The values represent a sum of spheroids in 10 optical fields under × 10 magnification. The results are mean ± S.E. from at least three experiments. Representative three-dimensional cultures are shown in Figs. 1 and 7.

Cells	Spheroids		
	25 ≤ 50 μm	50 ≤ 100 μm	>100 μm
MCF-7	21.0 ± 1.9	96.0 ± 6.7	2.7 ± 0.9
MCF-7/IGF-IR	1.7 ± 0.7	22.3 ± 1.4	86.5 ± 3.9
MCF-7/IGF-IR/anti-ZO-1	75.0 ± 3.5	40.7 ± 2.1	0.0 ± 0.0
MCF-7/Y3F	45.0 ± 2.9	39.8 ± 4.6	0.0 ± 0.0
MDA-MB-231	7.0 ± 0.6	0.5 ± 0.2	0.0 ± 0.0
MDA-MB-231/IGF-IR	12.5 ± 0.8	0.5 ± 0.1	0.0 ± 0.0
MDA-MB-231/E-cad	39.8 ± 3.6	15.2 ± 1.1	0.0 ± 0.0
MDA-MB-231/vector	10.0 ± 1.4	0.6 ± 0.4	0.0 ± 0.0
MDA-MB-231/IGF-IR/E-cad	27.0 ± 2.2	68.3 ± 7.2	8.0 ± 1.5
MDA-MB-231/IGF-IR/vector	18.6 ± 2.2	0.9 ± 0.3	0.0 ± 0.0

bind a target of Ras, AF6 (16). Deletions or mutations in the *ZO-1* gene produced overgrowth, suggesting that ZO-1 may act as a tumor suppressor (11). In breast cancer, ZO-1 is usually co-expressed with E-cad and is a strong independent marker of a more differentiated phenotype (17).

At present, very little is known about the regulation of ZO-1 by growth factors. However, some recent studies demonstrated that epidermal growth factor and vascular endothelial growth factor are able to increase ZO-1 tyrosine phosphorylation, modulate its subcellular localization, and consequently produce increased permeability (18–20). Here, we present the first evidence that in MCF-7 breast cancer cells 1) the IGF-IR up-regulates ZO-1 expression, 2) elevated levels of ZO-1 coincide with enhanced IGF-IR/E-cad-mediated cell-cell adhesion, and 3) ZO-1 expression is required for IGF-IR-increased cell aggregation in E-cad-positive MCF-7 cells.

MATERIALS AND METHODS

Expression Plasmids

E-cad Expression Plasmid—The pBAT-EM2 plasmid is a derivative of pBR322 and contains the mouse E-cad cDNA cloned under the β-actin promoter in pBR322 (21). As demonstrated previously, transfection of MDA-MB-231 cells with pBAT-EM2 results in E-cad overexpression, improved cell aggregation, and reduced metastatic potential of the cells (21, 22).

Antisense ZO-1 RNA Vector—The pcDNA3/anti-ZO-1 plasmid encoding the anti-ZO-1 antisense RNA contains a 959-base pair *Bam*HI fragment of the human ZO-1 cDNA (nucleotides 4205–5164) inserted (in the 3′-5′ orientation) into the pcDNA3.1/hygro plasmid (Invitrogen). pcDNA3/sense-ZO-1 is the control vector in which the above 959-base pair ZO-1 cDNA fragment was cloned in the 5′-3′ orientation.

Cell Lines and Cell Culture Conditions

MCF-7/IGF-IR clones 12, 15, and 17 are MCF-7-derived clones overexpressing the IGF-IR at the levels 5×10^5, 3×10^6, and 1×10^6 receptors/cell, respectively (7). To avoid clonal variation, in several experiments we used a population of mixed clones 12, 15, and 17. The mixed population is referred to as MCF-7/IGF-IR cells and expresses $\sim 0.9 \times 10^6$ IGF-IR receptors/cell (which represents ~18-fold overexpression over the levels in normal cells) (1). MCF-7/IGF-IR/Y3F express an IGF-IR ($\sim 3 \times 10^6$ receptors/cell) with inactivating mutations in the tyrosine kinase domain (Tyr-1131, Tyr-1135, and Tyr-1136 replaced with Phe) (23). MCF-7/IGF-IR/Y3F cells were derived from MCF-7 cells by stable transfection with the pcDNA3/IGF-IR/KR plasmid and subsequent selection in 2 mg/ml G418. The results obtained with the MCF-7/IGF-IR/Y3F clone were verified using a population of MCF-7 cells transiently transfected with the IGF-IR/Y3F vector (see below). MCF-7/IGF-IR/anti-ZO-1 and MCF-7/IGF-IR/sense ZO-1 cells were derived from MCF-7/IGF-IR clone 15 by stable transfection with the antisense and sense ZO-1 vectors, respectively and subsequent selection in 500 μg/ml hygromycin B.

MDA-MB-231 is a metastatic breast cancer cell line lacking E-cad and expressing $\sim 7 \times 10^3$ IGF-IR receptors/cell (24).[2] MDA-MB-231/IGF-IR clone 31 was derived from MDA-MB-231 cells by stable transfection with the pcDNA3/IGF-IR plasmid. MDA-MB-231/IGF-IR cells express ~250,000 IGF-IR/cell.[2]

All cell lines were grown in Dulbecco's modified Eagle's medium/F12 (1:1) containing 5% calf serum. MCF-7- and MDA-MB-231-derived clones transfected with the wild-type or mutant IGF-IR were maintained in growth medium with 100 μg/ml G418. MCF-7/IGF-IR/anti-ZO-1 and MCF-7/IGF-IR/sense ZO-1 cells were cultured in growth medium with 50 μg/ml hygromycin B. In the experiments requiring serum-free conditions, the cells were cultured in phenol red-free Dulbecco's modified Eagle's medium containing 0.5 mg/ml bovine serum albumin, 1 μM $FeSO_4$, and 2 mM L-glutamine (referred to as SFM).

Transient Transfection

MDA-MB-231 and MDA-MB-231/IGF-IR cells were transiently transfected using LipofectAMINE 2000 (Life Technologies, Inc.) (reagent/DNA ratio, 5 μl/1 μg). The transfection was carried out in growth medium for 24 h, and then the cells were lysed and processed for E-cad Western blotting (WB). To evaluate the extent of cell-cell adhesion in the transfected MDA-MB-231 and MDA-MB-231/IGF-IR cells, the cells were trypsinized upon transfection, counted, and placed in three-dimensional suspension culture as described below. MCF-7 cells were transfected for 6 h in growth medium using Fugene 6 (Roche Molecular Biochemicals) (reagent/DNA ratio, 3 μl/1 μg). To study IGF-I signaling, the transfected MCF-7 cells were shifted to SFM for 36 h and stimulated with IGF-I for 15 min. The efficiency of transfection (transfected cells/total cell number) was at least 70% for all cell types and was estimated by scoring fluorescent cells in cultures transfected with the plasmid pCMS (encoding green fluorescent protein) (Invitrogen).

Three-dimensional Spheroid Culture

The cells were grown to 70–80% confluence, trypsinized, and plated in single-cell suspension in 2%-agar-coated plates containing either normal growth medium or SFM. 2×10^6 cells were plated per 100 mm culture dish. To generate three-dimensional spheroids, the plates were rotated for 4 h at 37 °C. The spheroids started to assemble at ~1 h after plating and were completely organized after 3–4 h of culture in suspension. The three-dimensional cultures were photographed using a phase-contrast microscope (Nikon or Olympus). The extent of aggregation was scored by measuring the spheroids with an ocular micrometer. For each cell type, the spheroids between 25 and 50, 50 and 100, and >100 μm (in the smallest cross-section) were counted in 10 different fields under × 10 magnification.

IGF Stimulation

70% confluent cell cultures were synchronized in SFM for 36 h and then stimulated with 20 ng/ml IGF-I for 0–72 h.

Immunoprecipitation and Western Blotting

The expression of different elements of the adhesion complex was assessed in 500 μg of protein lysate by immunoprecipitation and WB

[2] Bartucci, M., Morelli, C., Mauro, L., Ando', S., and Surmacz, E. (2001) *Cancer Res.* **61,** 6747–6754.

with appropriate antibodies. The expression of ERK1/ERK2 was tested in 50 μg of total cell lysate. The cell lysis buffer contained 50 mM HEPES, pH 7.5, 150 mM NaCl, 1% Triton X-100, 1.5 mM $MgCl_2$, 1 mM $CaCl_2$, 100 mM NaF, 0.2 mM Na_3VO_4, 1% phenylmethylsulfonyl fluoride, and 1% aprotinin as described before (25). The following antibodies were used: anti-ZO-1 polyclonal antibody (pAb) (Zymed Laboratories Inc.) for ZO-1 immunoprecipitation (5 μg/ml) and WB (2 μg/ml); anti-E-cad monoclonal antibody (mAB), clone 36 (Transduction Laboratories) for E-cadherin immunoprecipitation (2 μg/ml) and WB (0.1 μg/ml); anti-α-catenin pAb (Sigma or Zymed Laboratories Inc.) for α-catenin immunoprecipitation (4 μg/ml) and WB (anti-serum dilution 1:4000); anti-β-catenin mAb (Transduction Laboratories) for β-catenin immunoprecipitation (4 μg/ml) and WB (0.5 μg/ml); anti-γ catenin pAb (Sigma) for γ-catenin WB (1 μg/ml); anti-actin mAb clone AC-40 (Sigma) for actin WB (0.4 μg/ml); anti-IGF-IR mAb, clone αIR-3 (Calbiochem) for IGF-IR immunoprecipitation (3 μg/ml), and anti-IGF-IR pAb C-20 (Santa Cruz Biotechnology) for IGF-IR WB (0.2 μg/ml); anti-p85 pAb (Upstate Biotechnology, Inc.) for the p85 subunit of the phosphatidylinositol 3-kinase WB (0.25 μg/ml); anti-phospho-MAPK mAb (New England Biolabs, Inc.) for active ERK1/ERK2 WB (0.5 μg/ml); and anti-MAPK pAb (New England Biolabs) for total ERK1/ERK2 WB (1 μg/ml). Tyrosine phosphorylation of immunoprecipitated proteins was measured by WB with anti-phosphotyrosine mAb (Transduction Laboratories) (0.03 μg/ml). Western blots were developed using an ECL chemiluminescence kit (Amersham Pharmacia Biotech). The intensity of bands representing relevant proteins was measured by laser densitometry scanning.

RESULTS

IGF-IR Overexpression Stimulates Cell-Cell Adhesion through an E-cad-dependent Mechanism—First, we demonstrated that under three-dimensional culture conditions, overexpression of the IGF-IR stimulated cell-cell adhesion in E-cad-positive MCF-7 breast cancer cells but not in E-cad-negative MDA-MB-231 cells (Fig. 1, *A* and *B*) (Table I). However, coexpression of the IGF-IR and E-cad resulted in robust cell-cell adhesion of MDA-MB-231 cells, whereas the expression of E-cad alone was less efficient in inducing intercellular contacts (Fig. 1, *C* and *D*) (Table I). These results, together with our previous data showing that IGF-IR-mediated aggregation in MCF-7 cells is blocked with an anti-E-cad antibody (7), indicated that IGF-IR adhesion signals are transmitted through the E-cad complex.

IGF-IR Overexpression Up-regulates ZO-1—We tested whether high levels of the IGF-IR affect the expression of the proteins within the E-cad complex and found that in MCF-7 and MCF-7/IGF-IR cells cultured as three-dimensional spheroids, the levels of E-cad and α-, β-, and γ-catenin were similar. However, the abundance of ZO-1 was significantly increased in MCF-7/IGF-IR cells (Fig. 2). The tyrosine phosphorylation of all these adhesion proteins was undetectable in spheroids and was not influenced by IGF-IR overexpression (Fig. 5 and data not shown).

To investigate whether the increased expression of ZO-1 in MCF-7/IGF-IR cells depends on IGF-IR tyrosine kinase activity, we generated by stable or transient transfection MCF-7/IGF-IR/Y3F cells expressing high levels of a kinase-defective IGF-IR mutant (IGF-IR/Y3F). The overexpression of the IGF-IR/Y3F mutant resulted in impaired IGF-I response, which was reflected by markedly reduced IGF-IR and IRS-1 tyrosine phosphorylation, decreased IRS-1/p85 binding, and diminished ERK1/ERK2 stimulation (Fig. 3). The basal expression of ZO-1 in MCF-7/IGF-IR/Y3F cells was significantly reduced compared with that in MCF-7/IGF-IR cells, indicating that tyrosine kinase activity of the IGF-IR is required for the up-regulation of ZO-1 (Fig. 3). Interestingly, the inhibition of IGF-I response did not affect E-cad expression, suggesting a selective action of the IGF-IR toward ZO-1 (Fig. 3). The blockade of the IGF-IR signal in MCF-7/IGF-IR/Y3F cells coincided with reduced cell-cell adhesion (Table 1).

ZO-1 mRNA and Protein Expression Is Regulated by IGF-I—To establish whether the activation of the IGF-IR by IGF produces a similar effect on ZO-1 as that seen with IGF-IR overexpression, we studied ZO-1 mRNA and protein in MCF-7 and MCF-7/IGF-IR cells treated with 20 ng/ml IGF-I for 1–72 h (Fig. 4). In MCF-7 cells cultured in SFM, the basal levels of ZO-1 mRNA were low and were markedly increased between 4 and 36 h of IGF-I treatment (Fig. 4*A*). In contrast, the abundance of ZO-1 mRNA was always elevated in MCF-7/IGF-IR cells and was only moderately improved by IGF-I (4–72 h) (Fig.

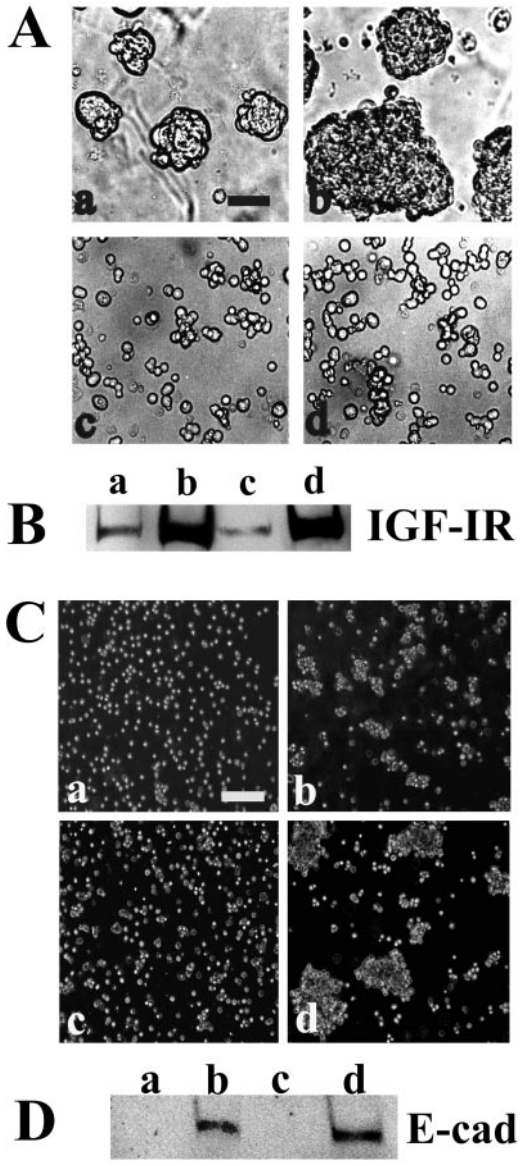

FIG. 1. **IGF-IR overexpression stimulates cell-cell adhesion in E-cad-positive but not in E-cad-negative breast cancer cells.** *A*, E-cad-positive MCF-7 and MCF-7/IGF-IR cells and E-cad-negative MDA-MB-231 and MDA-MB-231/IGF-IR cells were cultured in normal growth medium as three-dimensional spheroids for 24 h as described under "Materials and Methods" and then photographed under phase contrast microscopy. *a*, MCF-7 cells expressing ~6×10^4 IGF-IR/cell (7); *b*, MCF-7/IGF-IR, clone 12 expressing ~5×10^5 IGF-IGF-IR/cell (7); *c*, MDA-MB-231 cells with ~7×10^3 IGF-IGF-IR/cell (24), and *d*, MDA-MB-231/IGF-IR, clone 31 with ~3×10^5 IGF-IR/cell.[2] The *bar* in *a* equals 50 μm. *B*, IGF-IR levels in cells pictured in Fig. 1*A*, *a–d* were assessed by WB in 50 μg of cell lysate as described under "Materials and Methods." *C*, MDA-MB-231 and MDA-MB-231/IGF-IR cells were transiently transfected with the E-cad expression plasmid (*b* and *d*) or a vector alone (*a* and *c*) and then cultured in suspension as three-dimensional spheroids. The *bar* in *a* equals 100 μm. *D*, E-cad levels in cells pictured in Fig. 1*C*, *a–d* were determined by WB in 50 μg of cell lysate, as described under "Materials and Methods."

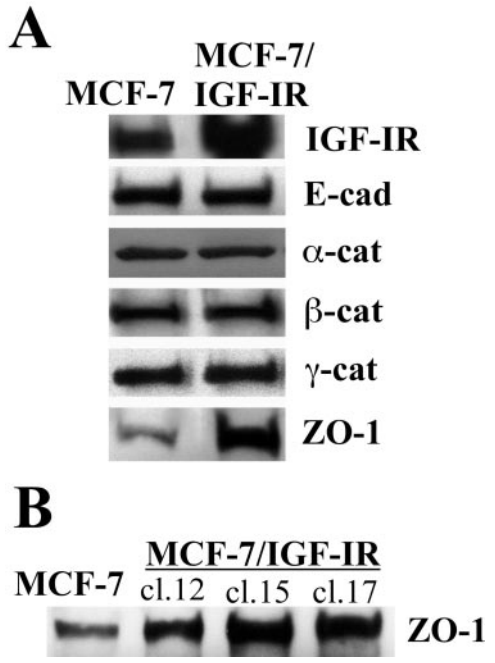

FIG. 2. **Expression of adhesion proteins in MCF-7 and MCF-7/IGF-IR cells.** The expression of adhesion proteins and the IGF-IR was studied in 50 μg of protein lysates obtained from cells cultured as three-dimensional spheroids in normal growth medium. MCF-7/IGF-IR cells are pooled MCF-7/IGF-IR clones 12, 15, and 17 (see "Materials and Methods"). *A*, the levels of the IGF-IR; E-cad; α-, β-, γ-catenin (*cat*); and ZO-1 detected by WB using specific antibodies (see "Materials and Methods"). *B*, the expression of ZO-1 in MCF-7 cells and in MCF-7/IGF-IR clones (*cl.*) 12, 17, and 15, expressing ~5×10^5, 1×10^6, and 3×10^6 IGF-IR/cell, respectively (7).

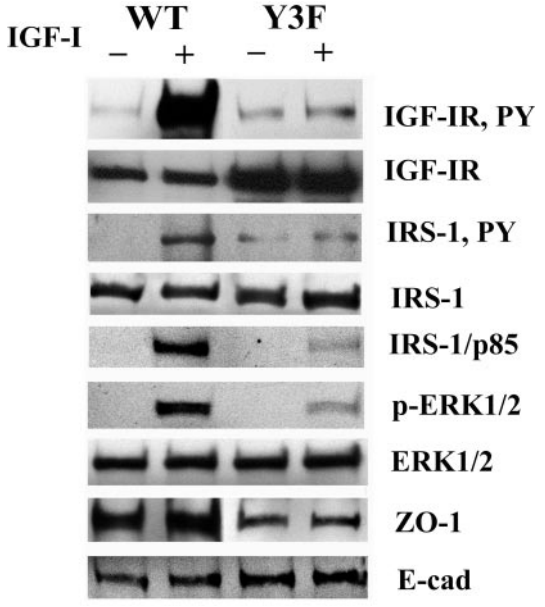

FIG. 3. **ZO-1 expression is inhibited in MCF-7/IGF-IR/Y3F cells.** MCF-7/IGF-IR cells expressing the wild-type IGF-IR (*WT*) and MCF-7/IGF-IR/Y3F cells stably transfected with a dominant-negative kinase-defective IGF-IR mutant (*Y3F*) were synchronized in SFM for 36 h and then stimulated for 15 min with 20 ng/ml IGF-I as described under "Materials and Methods." The expression and tyrosine phosphorylation (*PY*) of the IGF-IR and IRS-1 in the cells were detected by immunoprecipitation and WB in 500 μg of protein lysates. The binding of the p85 subunit of the phosphatidylinositol 3-kinase to IRS-1 (IRS-1/p85) was studied by WB in IRS-1 immunoprecipitates. The expression of active ERK1/ERK2 (p-ERK1/2), total ERK1/2, ZO-1, and E-cad was evaluated by WB in 50 μg of total protein lysates. The specific antibodies used are listed under "Materials and Methods." Similar results were obtained with MCF-7 cells transiently transfected with the IGF-IR/Y3F expression vector.

4*A*). ZO-1 protein levels in IGF-I-treated cells generally reflected the expression of ZO-1 mRNA (Fig. 4*B*).

Interactions of ZO-1 with the E-cad Complex in MCF-7/IGF-IR Cells—It has been recently reported that ZO-1 is an element of the E-cad complex (12–14). This complex also contains the IGF-IR, as described in our previous work (7, 8). Here, we analyzed tyrosine phosphorylation status of the IGF-IR, E-cad, and ZO-1, and the interactions among these proteins in MCF-7 and MCF-7/IGF-IR cells cultured as three-dimensional spheroids (Fig. 5). The autophosphorylation of the IGF-IR was elevated in MCF-7/IGF-IR cells, reflecting the increased responsiveness of the cells to IGF-IR ligands (IGF-I, IGF-II, and insulin) present in serum. However, tyrosine phosphorylation of E-cad and ZO-1 were unaffected by IGF-IR overexpression (Fig. 5*A*). Similarly, high levels of the IGF-IR did not affect tyrosine phosphorylation of α-, β-, or γ-catenin (data not shown). Next, we asked whether hyperactivation of the IGF-IR and increased expression ZO-1 have consequences for the associations among the proteins within the E-cad complex. Co-immunoprecipitation experiments demonstrated that IGF-IR overexpression resulted in an increased abundance of IGF-IR·E-cad and IGF-IR·ZO-1 complexes (Fig. 5*A*). Also, the elevated levels of ZO-1 in MCF-7/IGF-IR cells coincided with an increased association of ZO-1 with either E-cad or the IGF-IR (Fig. 5*A*). Moreover, the binding of α-catenin (a ZO-1-associated protein) to the IGF-IR or ZO-1 but not to E-cad was greater in MCF-7/IGF-IR cells than in MCF-7 cells (Fig. 5*A*). The presence of α-catenin in IGF-IR immunoprecipitates was confirmed with cell lysates in which α-catenin was first removed with a specific antibody. As expected, immunoprecipitation of such depleted lysates with either anti-IGF-IR or anti-E-cad antibodies revealed reduced α-catenin/E-cad and α-catenin/IGF-IR associations (Fig. 5*B*). Further experiments with α-catenin immunoprecipitates indicated increased abundance of α-catenin·actin and α-catenin·ZO-1 complexes in MCF-7/IGF-IR cells (Fig. 5*C*). A hypothetical model of possible interactions between adhesion proteins and the IGF-IR is shown in Fig. 6.

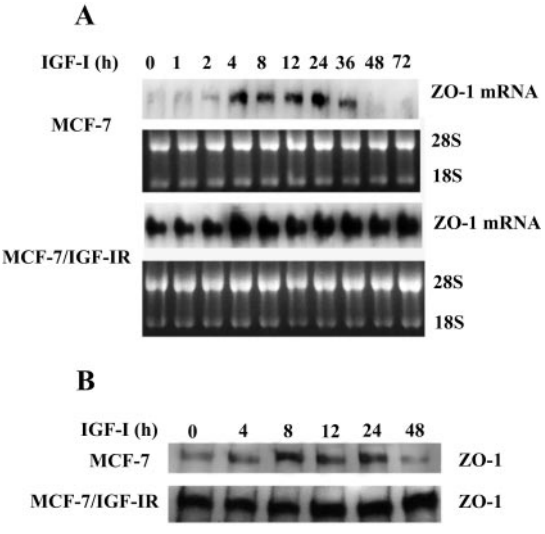

FIG. 4. **ZO-1 mRNA and protein are regulated by IGF-I.** *A*, MCF-7 cells and MCF-7/IGF-IR were synchronized in SFM (time 0) and then stimulated with 20 ng/ml IGF-I for different times (1–72 h). The expression of 7.8-kilobase ZO-1 mRNA in MCF-7 and MCF-7/IGF-IR cells was studied by Northern blotting in 20 μg of total RNA using a [^{32}P]dCTP-labeled ZO-1 probe (described under "Materials and Methods"). 28 and 18 S rRNA are shown as a control of RNA loading. *B*, the expression of ZO-1 protein in IGF-I-treated cells was detected by WB as described under Fig. 3.

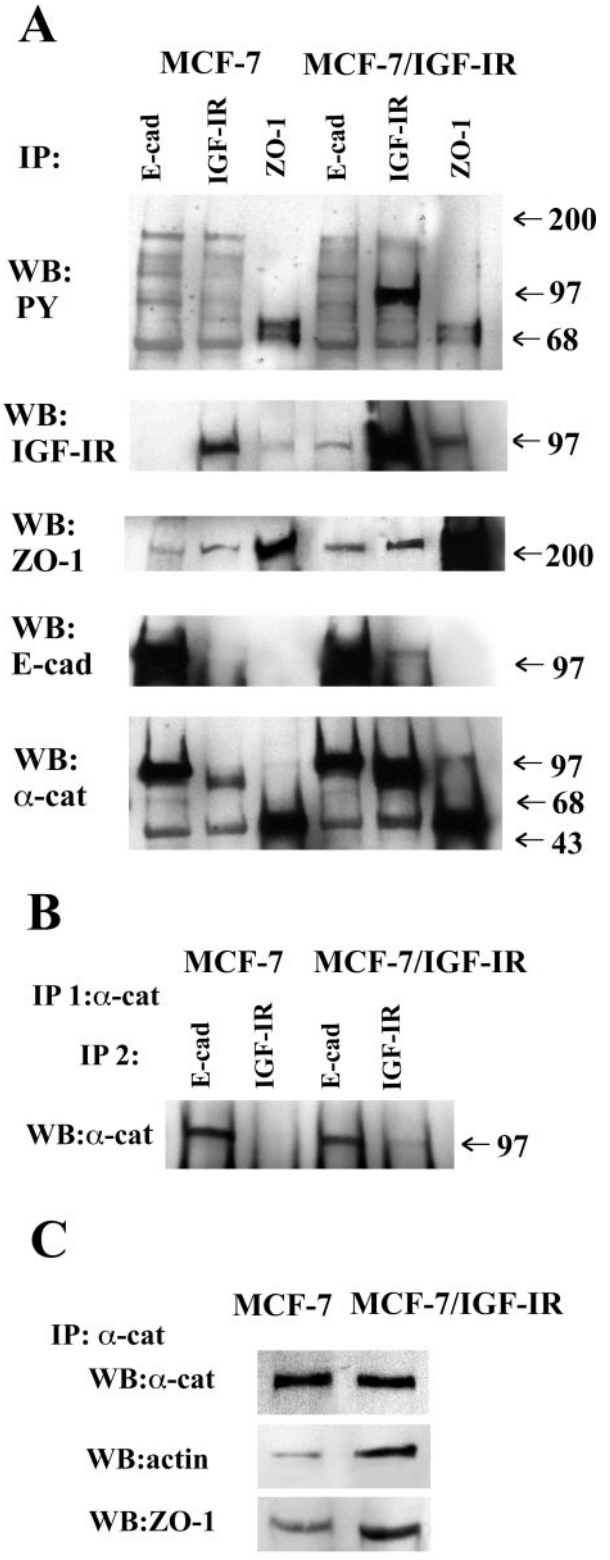

FIG. 5. **Interactions of ZO-1 with the IGF-IR in the E-cad complex.** *A*, the IGF-IR, E-cad, and ZO-1 were immunoprecipitated from 500 μg of total protein lysates obtained from MCF-7 and MCF-7/IGF-IR cells cultured as three-dimensional spheroids in normal growth medium. The immunoprecipitates (*IP*) were then probed by Western blotting (*WB*) for phosphotyrosine (*PY*), the IGF-IR (~97 kDa), ZO-1 (~220 kDa), E-cad (~120 kDa), and α-catenin (~102 kDa). *B*, to confirm α-catenin presence in IGF-IR immunoprecipitates, the lysates were first treated with anti-α-catenin antibodies (Zymed Laboratories Inc.) overnight to deplete α-catenin and then immunoprecipitated with either anti-E-cad or anti-IGF-IR antibodies. The E-cad and IGF-IR immunoprecipitates were then probed with another anti-α-catenin antibody (Sigma). Note significantly reduced α-catenin associations with IGF-IR and E-cad compared with that seen in *A*. *C*, 500 μg of protein lysates were precipitated with anti-α-catenin antibody and probed by WB for α-catenin, actin, and ZO-1. The blots presented in *A*, *B*, and *C* were identically developed with film exposure time 10 s.

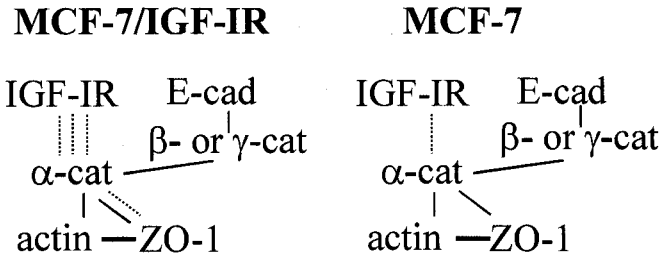

FIG. 6. **Possible interactions between ZO-1 and the IGF-IR within the E-cad complex.** The well established connections between E-cad, catenins, and actin are shown as *solid lines*. The proposed connections between the IGF-IR, α-catenin, ZO-1, and actin are drawn as *broken lines*. At present, it is not known whether the IGF-IR interacts with α-catenin directly or if other intermediate proteins are involved.

Down-regulation of ZO-1 Results in Decreased Cell-Cell Adhesion in MCF-7/IGF-IR Cells—Because the results suggested that ZO-1 may be an important intermediate in IGF-IR-stimulated cell-cell adhesion, we set out to confirm this notion using MCF-7/IGF-IR cells in which ZO-1 levels were down-regulated by the expression of an anti-ZO-1 RNA (MCF-7/IGF-IR/anti-ZO-1 cells) (Fig. 7). The clones with the best ZO-1 reduction and an intact E-cad and IGF-IR expression were analyzed in three-dimensional culture. The cell-cell adhesion of MCF-7/IGF-IR/anti-ZO-1 cells was greatly inhibited compared with that in the parental MCF-7/IGF-IR cells (Fig. 7 and Table 1). The expression of the anti-ZO-1 plasmid in the parental MCF-7 cells was toxic, and no viable clones were obtained. The transfection of the sense-ZO-1 vector had no effect on cell-cell adhesion (data not shown).

DISCUSSION

Cell-cell adhesion is a known factor modulating the motility of tumor cells and consequently impacting tumor metastasis (26). The regulation of this process by exogenous growth factors is still not well understood. In E-cad-positive breast cancer cells, the overexpression or activation of the IGF-IR has been shown to stimulate cell-cell adhesion and reduce cell spreading *in vitro* or in organ culture (7–10). The IGF-IR has also been found co-localized and co-precipitated with the E-cad adhesion complex (7, 8). The mechanism of IGF-IR-stimulated E-cad-dependent cell-cell adhesion is unknown and has been investigated in this work. We discovered the following observations. 1) IGF-IR overexpression increased aggregation in E-cad-positive cells but not in E-cad-negative cells. 2) High expression of both IGF-IR and E-cad markedly improved cell aggregation in E-cad-negative cells. 3) IGF-IR-dependent cell-cell adhesion in E-cad-positive cells did not affect the expression of E-cad or α-, β-, or γ-catenins but coincided with up-regulation of ZO-1. 4) ZO-1 expression was induced by IGF-I and required IGF-IR tyrosine kinase activity, and 5) high levels of ZO-1 coincided with an increased IGF-IR/α-catenin/ZO-1 binding and improved ZO-1/actin association, whereas down-regulation of ZO-1 by the expression of an anti-ZO-1 RNA inhibited IGF-IR-dependent cell-cell adhesion. We hypothesize that the mechanism or one of the mechanisms by which the activated IGF-IR stimulates cell-cell adhesion is overexpression of ZO-1 and the resultant stronger connections between the E-cad complex and the actin cytoskeleton.

Very little is known about the regulation of ZO-1 by growth

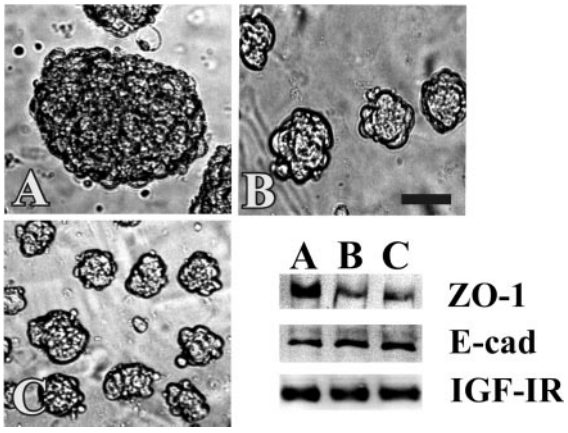

FIG. 7. **Reduced cell-cell adhesion in MCF-7/IGF-IR/anti-ZO-1 cells.** MCF-7/IGF-IR/anti-ZO-1 clones were obtained by stable transfection of MCF-7/IGF-IR cells with an anti-ZO-1 RNA expression plasmid (see "Materials and Methods"). The levels of ZO-1, IGF-IR, and E-cad in the parental MCF-7/IGF-IR cells (*A*) and in the clones (*B* and *C*) were studied by WB in 50 μg of protein lysate. The aggregation of cells was studied in three-dimensional culture as described under "Materials and Methods." The *bar* in *B* represents 50 μm.

factors. Several growth factors (*e.g.* epidermal growth factor and vascular endothelial growth factor) have been demonstrated to increase tyrosine phosphorylation of ZO-1 in different cellular model systems (18, 19). Hyperphosphorylation of ZO-1 usually coincides with its departure from tight junctions into the cytoplasm and with increased permeability (18, 19). In addition, v-Src-increased ZO-1 tyrosine phosphorylation has been linked to decreased cell-cell adhesion (27). IGF-I, on the other hand, has been shown to stabilize ZO-1 in tight junctions and to preserve the epithelial barrier in embryonic kidney cells and in pig thyrocytes (28, 29). However, the effects of IGF-I on ZO-1 expression and function in breast cancer cells have never been explored. Our findings provide the first evidence that the activation of the IGF-IR up-regulates ZO-1 mRNA and protein levels without affecting ZO-1 tyrosine phosphorylation. Consistent with the results obtained in other models, we noted increased adhesion in cells overexpressing ZO-1 and reduced aggregation in cells with down-regulated ZO-1 levels.

IGF-IR tyrosine phosphorylation was required for the stimulation of ZO-1 expression, inasmuch as the basal levels of ZO-1 were not increased in MCF-7/IGF-IR/Y3F cells expressing a dominant-negative, kinase-defective mutant of the IGF-IR. However, the putative IGF-I signaling pathways leading to ZO-1 expression have yet to be characterized. Our preliminary data with MCF-7/IRS-1 cells, in which the major IGF-IR/IRS-1/phosphatidylinositol 3-kinase growth/survival pathway is hyperactivated (1), suggested that this pathway is not involved in ZO-1 regulation (data not shown).

The clinical implications of IGF-induced and ZO-1-mediated cell-cell adhesion on tumor development and progression are unknown. Until now, the data from our and other laboratories suggest that in E-cad-positive breast cancer cells IGF-IR improves cell-cell adhesion and cell survival in three-dimensional culture but at the same time reduces cell spreading (1). Thus, one consequence of IGF-IR overexpression in breast cancer could be increased growth and survival of the primary tumor but reduced cell metastasis. This hypothesis is consistent with the observation that the IGF-IR is a good prognostic indicator for breast cancer, as tumors with good prognosis express much higher levels of the IGF-IR than tumors with bad prognosis (1, 30, 31). Notably, an independent study has shown that in breast tumors, E-cad and ZO-1 are co-expressed and are markers of a more differentiated phenotype (17). A formal analysis of the correlations between ZO-1 and the IGF-IR is underway in our laboratory and should help in clarifying the role of the IGF-IR in breast cancer progression.

Acknowledgments—Drs. J. M. Anderson and A. S. Fanning (Yale University, New Haven, CT) generously provided the pSKZO-1 plasmid encoding the human ZO-1 cDNA. The E-cad expression vector pBAT-EM2 was a gift from Drs. M. Takeichi (Kyoto University, Kyoto, Japan) and T. Yoneda (University of Texas, San Antonio, TX). The MCF-7/Y3F clone was developed by Dr. M. Guvakova (University of Pennsylvania, Philadelphia, PA).

REFERENCES

1. Surmacz, E. (2000) *J. Mamm. Gland Biol. Neoplasia* **5,** 95–105
2. Werner, H., and Le Roith, D. (2000) *Cell. Mol. Life Sci.* **57,** 932–942
3. Baserga, R. (1999) *Exp. Cell Res.* **253,** 1–6
4. Resnik, J. L., Reichart, D. B., Huey, K., Webster, N. J. G., and Seely, B. L. (1998) *Cancer Res.* **58,** 1159–1164
5. Dunn, S. E., Ehrlich, M., Sharp, N. J. H., Reiss, K., Solomon, G., Hawkins, R., Baserga, R., and Barrett, J. C. (1998) *Cancer Res.* **58,** 3353–3361
6. Doerr, M., and Jones, J. J. (1996) *Biol. Chem. Hoppe-Seyler* **271,** 2443–2447
7. Guvakova, M. A., and Surmacz, E. (1997) *Exp. Cell Res.* **231,** 149–162
8. Surmacz, E., Guvakova, M., Nolan, M., Nicosia, R., and Sciacca, L. (1998) *Breast Cancer Res. Treat.* **47,** 255–267
9. Bracke, M. E., Vyncke B. M., Bruyneel, E. A., Vermeulen, S. J., De Bruyne, G. K., Van Larebeke, N. A., Vleminckx, K., Van Roy F. M., and Mareel, M. M. (1993) *Br. J. Cancer* **68,** 282–289
10. Bracke, M. E., Van Roy, F. M., and Mareel, M. M. (1996) *Curr. Top. Microbiol. Immunol.* **213,** 123–161
11. Willott, E., Balda, M. S., Fanning, A. S., Jameson, B., Van Itallie, C., and Anderson, J. M. (1993) *Proc. Natl. Acad. Sci. U. S. A.* **90,** 7834–7838
12. Tsukita, S., Furuse, M., and Itoh, M. (1997) *Soc. Gen. Physiol. Ser.* **52,** 69–76
13. Itoh, M., Nagafuchi, A., Moroi, S., and Tsukita, S. J. (1997) *Cell Biol.* **138,** 181–192
14. Rajasekaran, A. K., Hojo, M., Huima, T., and Rodriguez-Boulan, E. J. (1996) *Cell Biol.* **132,** 451–463
15. Provost, E., and Rimm, D. L. (1999) *Curr. Opin. Cell Biol.* **11,** 567–572
16. Yamamoto, T., Harada, N., Kano, K., Taya, S., Canaani, E., Matsuura, Y., Mizoguchi, A., Ide, C., and Kaibuchi, K. J. (1997) *Cell Biol.* **139,** 785–795
17. Hoover, K. B., Liao, S.-Y., and Bryant, P. J. (1998) *Am. J. Pathol.* **153,** 1767–17773
18. Van Itallie, C. M., Balda, M. S., and Anderson, J. M. (1995) *J. Cell Sci.* **108,** 1735–1742
19. Antonetti, D. A., Barber, A. J., Hollinger, L. A., Wolpert, E. B., and Gardner, T. W. (1999) *J. Biol. Chem.* **274,** 23463–23467
20. Merwin, J. R., Anderson, J. M., Kocher, O., Van Itallie, C. M., and Madri, J. A. (1990) *J. Cell. Physiol.* **142,** 117–128
21. Nagafuchi, A., Shirayoshi, Y., Okazaki, K., Yasuda, K., and Takeichi, M. (1987) *Nature* **329,** 341–343
22. Mbalaviele, G., Dunstan, C. R., Sasaki, A., Williams, P. J., Mundy, G. R., and Yoneda, T. (1996) *Cancer Res.* **56,** 4063–4070
23. Kato, H., Faria, T., Stannard, B., Roberts, C. T., Jr., and LeRoith, D. (1994) *Mol. Endocrinol.* **8,** 40–50
24. Peyrat, J. P., Bonneterre, J., Dusanter-Fourt, I., Leroy-Martin, B., Dijane, J., and Demaille, A. (1989) *Bull. Cancer* (*Paris*) **76,** 311–319
25. Mauro, L., Sisci, D., Salerno, M., Kim, J., Tam, T., Guvakova, M., Ando, S., and Surmacz, E. (1999) *Exp. Cell Res.* **252,** 439–448
26. Christofori, G., and Semb, H. (1999) *Trends Biochem. Sci.* **24,** 73–76
27. Takeda, H., Nagafuchi, A., Yonemura, S., Tsukita, S., Behrens, J., Birchmeier, W., and Tsukita, S. (1995) *J. Cell Biol.* **131,** 1839–1847
28. Sakurai, H., Barros, E. J., Tsukamoto, T., Barasch, J., and Nigam, S. K. (1997) *Proc. Natl. Acad. Sci. U. S. A.* **94,** 6279–6284
29. Ericson, L. E., and Nilsson, M. (1996) *Eur. J. Endocrinol.* **135,** 118–127
30. Pezzino, V., Papa, V., Milazzo, G., Gliozzo, B., Russo, P., and Scalia, P. L. (1996) *Ann. N. Y. Acad. Sci.* **784,** 189–201
31. Schnarr, B., Strunz, K., Ohsam, J., Benner, A., Wacker, J., and Mayer, D. (2000) *Int. J. Cancer* **89,** 506–513

IGF-I Receptor-induced Cell-Cell Adhesion of MCF-7 Breast Cancer Cells Requires the Expression of Junction Protein ZO-1

Loredana Mauro, Monica Bartucci, Catia Morelli, Sebastiano Ando' and Eva Surmacz

J. Biol. Chem. 2001, 276:39892-39897.
doi: 10.1074/jbc.M106673200 originally published online August 22, 2001
